www.ietdl.org

Published in IET Microwaves, Antennas & Propagation
Received on 16th February 2012
Revised on 9th October 2012
Accepted on 9th November 2012
doi: 10.1049/iet-map.2012.0093

ISSN 1751-8725

Generating a pure circularly polarised axial beam from a pattern reconfigurable square loop antenna

Arpan Pal, Amit Mehta, Michel E. Marhic

College of Engineering, Swansea University, Swansea SA2 8PP, UK
E-mail: a.mehta@swan.ac.uk

Abstract: A pattern reconfigurable square loop antenna (SLA) is capable of generating tilted and doughnut beam patterns. In this study, it is demonstrated that the same antenna can be used to generate a circularly polarised axial beam if all four feeds are excited simultaneously with equal amplitude and a sequential phasing of 90°. Thus, the same square loop is capable of generating three distinct unit patterns by changing its feed excitation mechanism. This phenomenon makes the SLA an exceptional candidate for integration in the unit pattern reconfigurable antenna array. The study presents a complete design of SLA in conjunction with the feeding network and validates the computed and experimental results for a test band from 4.3 to 5 GHz. The antenna provides an axial beam of a maximum directivity of 7.4 dBi over the test band and yields near to ideal circular polarisation at broadsight. Using current distributions an explanation for the mechanism of generation of circularly polarised axial beam is also presented.

1 Introduction

Pattern reconfigurable antennas have received much attention in wireless communications technology, mobile satellite communication, radars and global positioning systems to meet the requirements for ever-increasing functionality and data capacity. Reconfigurable antennas with the ability to generate multiple patterns are set to become a crucial part in modern communication systems since they direct the beam only towards the intended direction of signal arrival and evade the noise sources, resulting in a higher *S*/*N* system with higher data throughput capacity.

Single element reconfigurable antennas are of special significance as they do not require multiple antenna elements as a conventional phase array antenna does [1, 2]. Thus, for portable devices with limited size single element steerable antennas are the way forward. Different types of architectures have been investigated [3–11] to realise the steerable antennas that can be operated over a wide bandwidth. These antennas employed multiple switches to vary the current distribution along the peripheral length for achieving reconfigurable radiation patterns. Owing to the different current distribution the antenna polarisation differs from one switching configuration to another and causes polarisation randomness.

Planar square loop antenna (SLA) has been proposed for switched beam steering applications [7–9] which use their structural symmetry in order to achieve reconfigurable radiation pattern without any polarisation variation from one pattern to another. The SLA has four input ports and when it is excited through one of its ports, it generates a tilted beam directed towards the opposite of the active port. The SLA can steer its beam to four quadrants in space in front of antenna using an RF switch, which directs the input RF power to one of the four input ports of the antenna [11]. The original SLA [7] antenna was on a thick substrate and suffered from a narrow impedance bandwidth. These drawbacks were tackled and resolved by using hybrid high impedance surface (HHIS) [9]. It has been reported that SLA can also provide doughnut pattern beam when all the four feeds are excited by RF signals of equal amplitude and same phase [12]. Nevertheless, so far these SLA's can only generate a linearly polarised tilted beam or semi-doughnut pattern (dual unit patterns). Therefore these antennas are not suitable for the systems where signal may arrive from the axial direction or are circularly polarised (CP).

The recent interest of the antenna designer society is to develop antennas which can produce multiple types of unit patterns (three or more). In this paper for the first time it has been proposed that an SLA can also produce a CP axial beam when all the four feeds are powered simultaneously with equal amplitude and a sequential phase shift of 90°. Hence, enabling the SLA to provide three distinct unit patterns (tilted, semi-doughnut and axial). This property is of high significance from an array antenna implementation [13, 14] point of view. In conventional array antennas each individual element has single unit pattern and the assembly utilises the array factor to produce reconfigurable radiation patterns. However, the maximum directivity of an array antenna along a desired direction is limited by the directivity of the unit pattern. Therefore SLA capable of changing its unit pattern in such a way that it is always providing its main high gain beam in the direction of interest stands out as a special candidate.

Hence, besides having a tilted beam for communication from offbore-sight direction and semi-doughnut beam for sideways communications, which has been covered previously [12], this paper focuses on an HHIS-based SLA ability to generate a CP axial beam for communicating in the axial direction. This is achieved by simultaneously exciting four ports of SLA with signals of equal amplitude and a sequential phase shift of 90°. For this purpose a four way Wilkinson power divider/combiner along with delay transmission line for providing phase shifts were designed. A demonstrator antenna together with the feed network was simulated and fabricated to operate at the test frequency band of 4.3–5 GHz. The simulated and experimental reflection coefficient (S_{11}) and radiation patterns over the test frequency band are presented in the paper. Also, a brief theoretical explanation of the mechanism associated with the formation of CP axial beam is discussed using the current distributions. Note that the ability to generate CP beam is an additional bonus from SLA as it is useful to implement polarisation diversity in order to prevent degradation because of multipath fading and also allow more flexible orientation of the transmitter and receiver antennas [1].

2 Antenna configuration

Fig. 1 shows the top and side views of the HHIS-based SLA. The antenna structure is directly referred from [9]. In short, it has four conducting arms, each of length $l = 30$ mm and width $w = 1.5$ mm. From the bottom four ports (A, B, C and D) the antenna is excited at the centre points of each arm using four vertical SMA probes having a diameter of 1.3 mm. The HHIS structure is inserted between the top substrate (Rogers 4350B with dielectric constant $\varepsilon_{r1} = 3.48$ and thickness $h_1 = 1.52$ mm) and the bottom substrate (Rogers RT5880 with $\varepsilon_{r2} = 2.2$ and $h_2 = 3.17$ mm) each having an area, $L \times L = 60.3$ mm × 60.3 mm. The square loop is etched on the top substrate and the entire structure is backed by a metal conducting ground plane. The HHIS structure is composed of a 6 × 6 array of square metal patches. Each square has a side length of 8.8 mm with a gap of 1.5 mm between two neighbouring patches. The squares on the outer periphery of the HHIS structure are shorted to the ground by metal vias, each having a diameter of 3 mm. The vias are inserted only to the outermost patches to reduce the interaction between the square loop and the metal vias [9]. The outermost square patches of HHIS behave as one-dimensional grounded HIS and restrict the flow of surface waves. The remaining 4 × 4 array behaves as via-less HIS to enhance the impedance bandwidth and to provide a wide radiation bandwidth with reduced side lobes.

In [9], only one port of the SLA was excited at a time, whereas the other three were left as open circuits. That configuration gives a linearly polarised tilted beam directed away from the activated port. Now in this paper we show that when all the four ports (A, B, C and D) are excited simultaneously by RF signals having equal amplitudes and sequential clockwise phase delay of 90° ($\phi_A = 0°$, $\phi_B = 90°$, $\phi_C = 180°$ and $\phi_D = 270°$), the SLA generates a left-handed circularly polarised (LHCP) axial beam. It is worth pointing out that if the phase delay were anti-clockwise then the antenna would generate a right-handed circularly polarised (RHCP) axial beam. For satisfying these requirements (proof of concept) a feeding network using a four-way Wilkinson power divider/combiner and delay lines is designed and optimised. Fig. 2 shows the top view of the four-way power divider/combiner. This divides the main RF input power from port 1 equally into four at ports 2–5. The power divider with the delay lines are designed over a metal-backed Rogers's 4350B substrate having an area of 35 mm × 40 mm and thickness of 0.508 mm. The top view of power divider and delay line network is shown in Fig. 2.

A transmission delay line of length l introduce a phase shift $\theta = (l/\lambda_g) \times 360°$ (where, λ_g is the effective wavelength of the used substrate). The feed network was designed for test frequency of 4.7 GHz and the following dimensions were reached for achieving the necessary phase shift criteria: $l_1 = 9.65$ mm, $g_1 = 2$ mm, $l_2 = 9.85$ mm, $l_3 = 5$ mm, $l_4 = 5.8$ mm, $l_5 = 2$ mm, $l_6 = 2.34$ mm, $l_7 = 8.52$ mm, $l_8 = 4$ mm, $l_9 = 5.35$ mm, $l_{10} = 4.1$ mm, $l_{11} = 4.1$ mm, $l_{12} = 2.73$ mm, $l_{13} = 2.04$ mm, $l_{14} = 2.8$ mm, $l_{15} = 4.35$ mm, $l_{16} = 5.75$ mm, $l_{17} = 5.23$

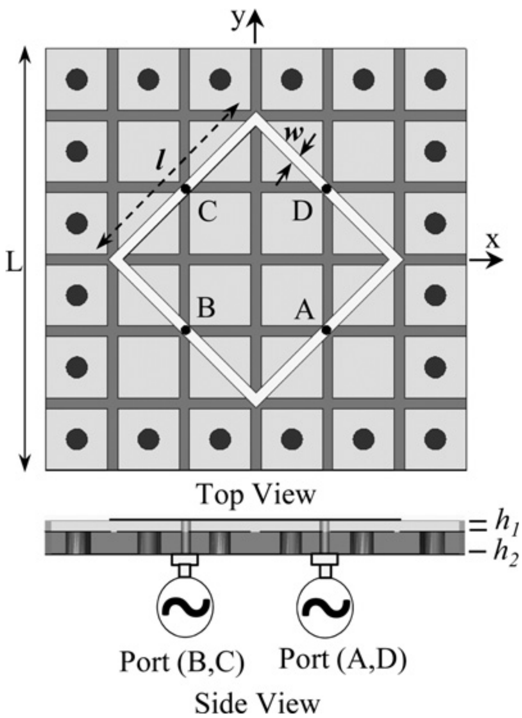

Fig. 1 *Top and side views of the HHIS-based SLA*

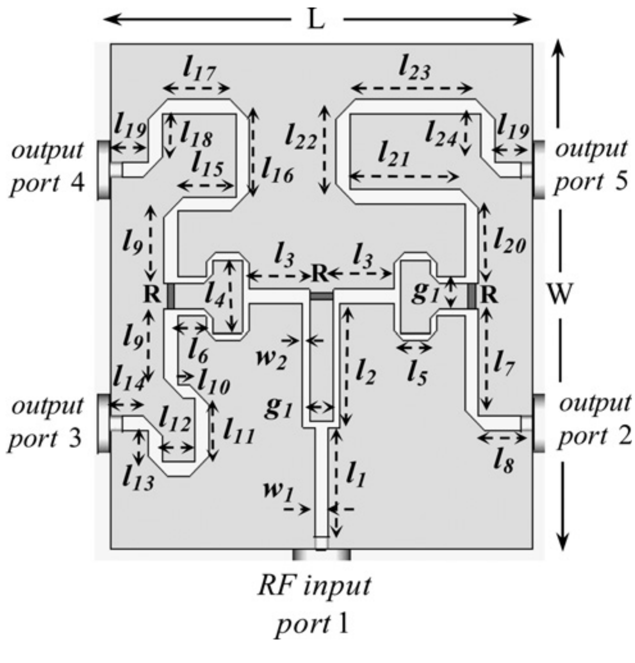

Fig. 2 *Top view of the four-way Wilkinson power divider with delay lines*

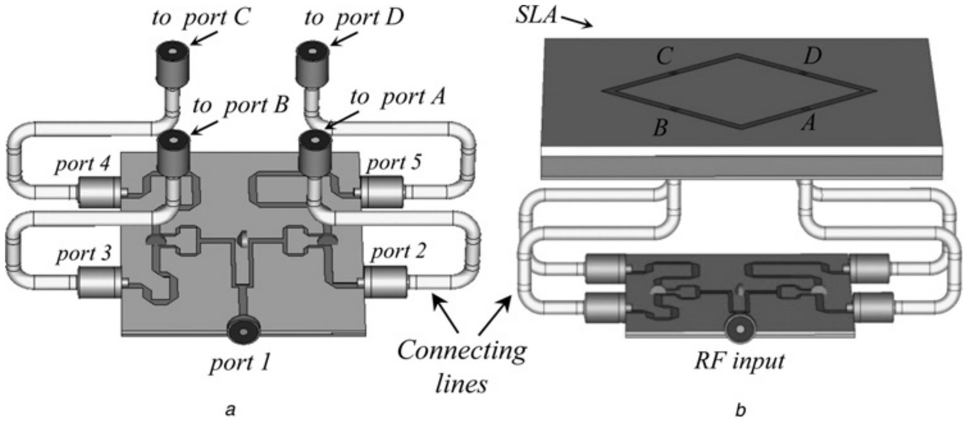

Fig. 3 *Perspective view*

a Feeding network with connecting feed lines
b SLA integrated with the feeding network

mm, $l_{18} = 3.48$ mm, $l_{19} = 3.18$ mm, $l_{20} = 5.95$ mm, $l_{21} = 9.13$ mm, $l_{22} = 5.15$ mm, $l_{23} = 9.98$ mm, $l_{24} = 3.48$ mm, $w_1 = 1.12$ mm, $w_2 = 0.56$ mm and $R = 100\ \Omega$.

The four ports of the antenna (A, B, C and D) are connected to the four output ports of the power divider (ports 2–5) by using four flexible connecting lines each having length of 50 mm and impedance of 50 Ω, as shown in Fig. 3. The lengths of the connecting lines are kept as small as possible (50 mm) to reduce the insertion loss and to avoid any probable pattern distortion which could have occurred if the connecting lines would have considerably spread beyond the antenna ground plane [11]. The antenna performance is simulated using CST microwave studio based on finite integration technique in time domain [15]. The radiation patterns are measured using Satimo's Star Laboratory [16] and the return losses using a vector network analyser.

3 Results and discussion

Fig. 4 shows the simulated frequency response of *s*-parameters and unwrapped phases at the four output ports of the feed network (Fig. 2). A wide band 1–4 Wilkinson power dividing network is realised with the aid of printed transmission lines of lengths as mentioned in section above for achieving the necessary phase shifting. As seen from Fig. 4, the reflection coefficient at port 1 (S_{11}) is <−10 dB

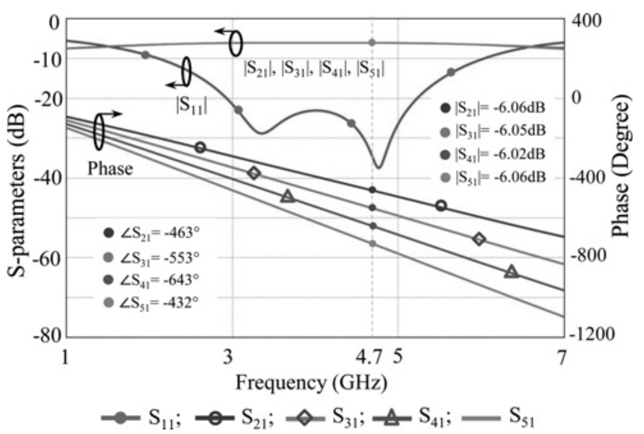

Fig. 4 *Frequency response of s-parameters and unwrapped phase at the output ports of the feed network (Fig. 2)*

and an equal power division to the four ports is achieved in the test band of 4.3–5 GHz. At 4.7 GHz each port receives nearly one-fourth of the input power, with $|S_{21}| = -6.06$ dB, $|S_{31}| = -6.05$ dB, $|S_{41}| = -6.02$ dB and $|S_{51}| = -6.06$ dB. Further, at the test frequency the unwrapped phase at port 2 is $\angle S_{21} = -463°$ and at port 3 is $\angle S_{31} = -553°$. Thus, the phase difference between ports 2 and 3 is $\angle S_{21} - \angle S_{31} = 90°$.

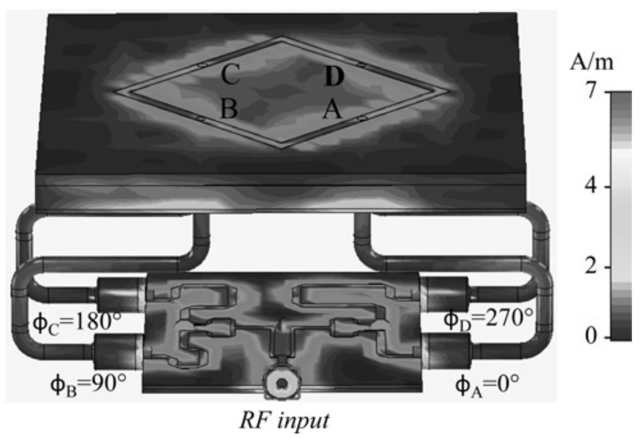

Fig. 5 *Computed average current distribution of the SLA integrated together with the feeding network*

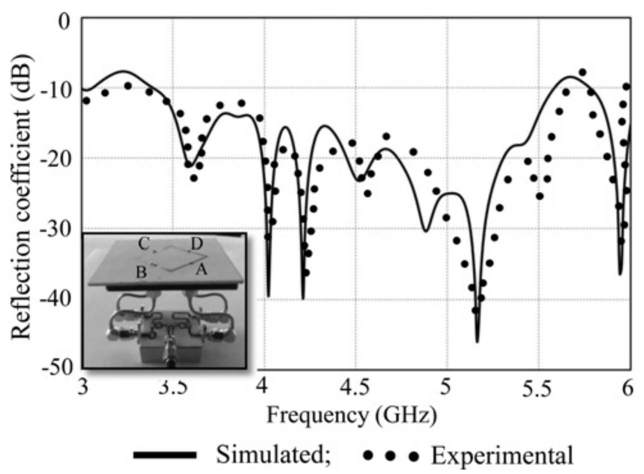

Fig. 6 *Computed and experimental reflection coefficient of SLA in conjunction with the feeding network*

(Inset) Experimental setup

Similarly, the phase differences between the output of ports 3 and 4 and that of ports 4 and 5 are also kept at 90°. Consequently, the feed network provides a clockwise sequential phase shift of 90° at four output ports and enables the antenna to provide CP radiation pattern. It is observed that although there was a ±5° error in sequential phase shift over the test frequency band the performance of the antenna was not significantly affected.

Fig. 5 shows the perspective view with current distribution of the SLA integrated with the feeding network for the RF input of 1 W. It can be seen that the power divider divides the input RF power equally into four parts and each signal travels a certain length along the delay lines to provide the appropriate phase shifts at output ports of the power divider. The frequency response of the computed and experimental reflection coefficient (S_{11}) of the SLA integrated with the feeding network is shown in Fig. 6. The experimental result is in close match with the simulation result. The antenna provides a wide bandwidth of 2.2 GHz (3.4–5.6 GHz) for −10 dB reflection coefficient criterion.

Fig. 7 shows the computed and experimental radiation patterns in *xz*-plane (ϕ = 0°) and *yz*-plane (ϕ = 90°) at 4.3, 4.7 and 5 GHz. The experimental radiation patterns are in close agreement with the computed patterns. It can be seen that the antenna features unidirectional LHCP beam and stable pattern over the test frequency band of 700 MHz.

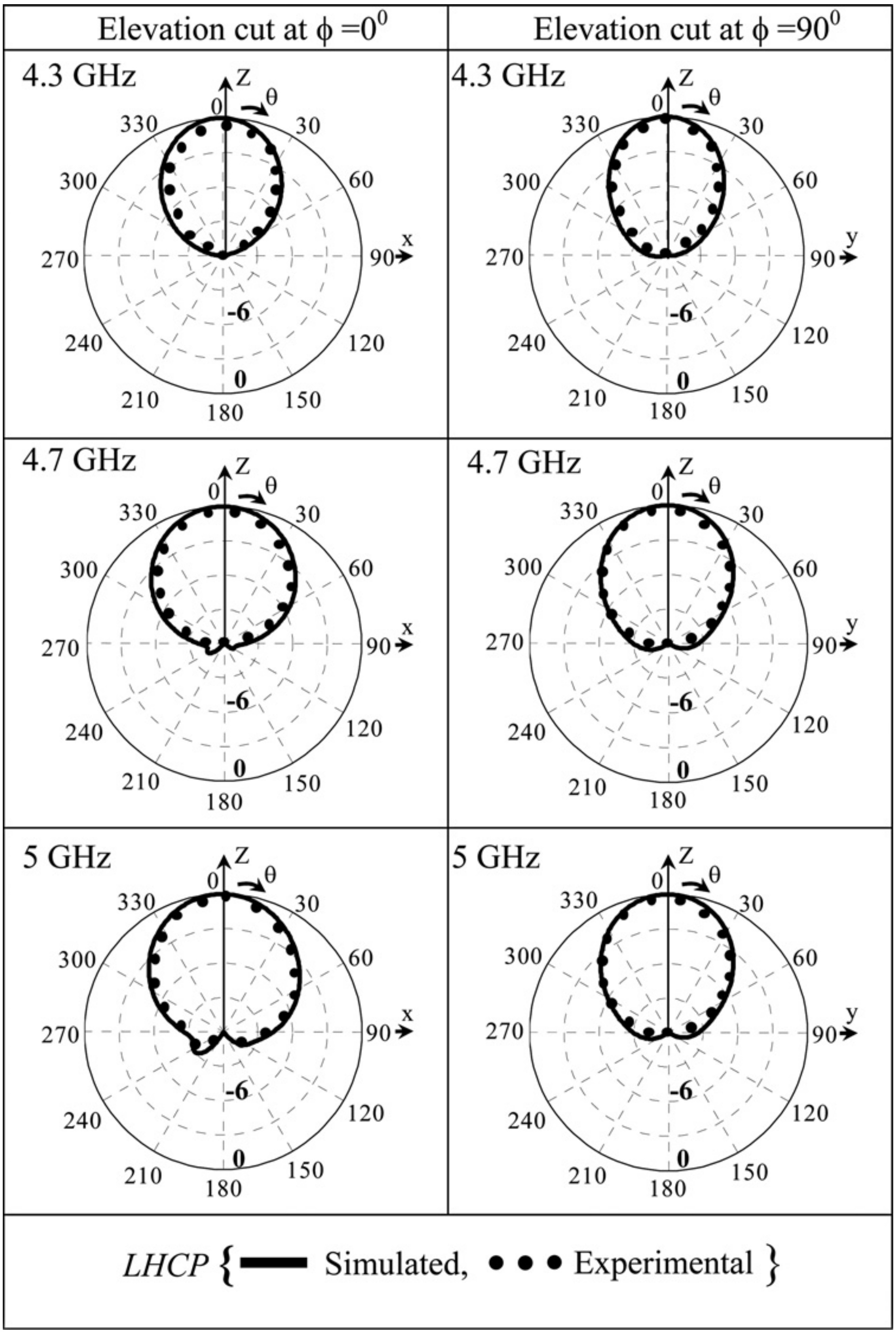

Fig. 7 *Computed and experimental normalised radiation patterns of SLA in the xz-plane (ϕ = 0°) and yz-plane (ϕ = 90°)*

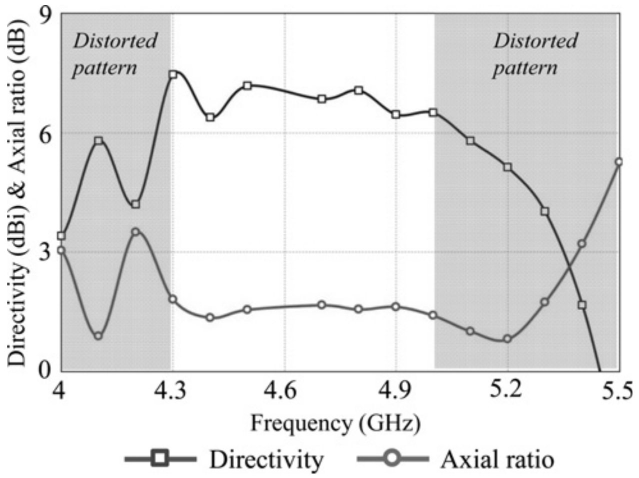

Fig. 8 *Directivity and axial ratio at θ = 0° and ϕ = 0° as a function of the frequency*

The level of cross polarisation (i.e. RHCP) is well below −15 dB over the main beam and front-to-back ratio is over 15 dB across the whole band. On the both sides of the test band the LHCP axial beam pattern starts to get distorted (the axial ratio >3 dB and side lobes start to get dominant) as shown in Fig. 8. This restricted axial ratio and pattern bandwidth are because of narrowband microstrip line feeding network in which the equal power division and sequential phasing criteria significantly deteriorates beyond the 700 MHz band. For the test band a directivity variation of 0.9 dB (7.3–6.4 dBi) was observed, with a near-linear reduction with frequency from 4.3 to 5.0 GHz.

4 Analysis using current distributions

In this section, we reveal the three current distributions which enable SLA to provide three distinct patterns, namely semi-doughnut [12], elliptically polarised axial beam and a CP axial beam, which is the focus of this paper. For this, it is assumed that when phase is zero the current travels in clockwise direction and when phase is of 180° the current travels in the counter-clockwise direction.

Fig. 9*a* shows the instantaneous current direction on the arms of SLA when all its four ports are excited simultaneously with a signal of same phase and amplitude ($\phi_A = 0°$, $\phi_B = 0°$, $\phi_C = 0°$ and $\phi_D = 0°$). Now with all arms with zero phases a clockwise current travels on the square loop. This means, arms A and C, and arms B and D have opposite current direction, respectively. This results in cancellation of electric fields at zenith ($z = 0$) which results in a semi-doughnut pattern [12] with a linearly polarised wave.

When the opposite arms of SLA are excited with a phase difference of 180° between them ($\phi_A = 0°$, $\phi_B = 0°$, $\phi_C = 180°$ and $\phi_D = 180°$), Fig. 9*b*, then arms A and B have clockwise current, and arms C and D have counter clockwise. Therefore opposite arms have current in the same direction which results in two orthogonal fields (horizontal = *H* and vertical = *V*) which add up in zenith, and hence produce an axial beam. For instance, arms A and C radiate a *V* component and arms B and D radiate an *H* component, and phase shifts of 180° between them results in an elliptically polarised radiation.

Finally, in Fig. 9*c* when the four arms are fed with sequential delay ($\phi_A = 0°$, $\phi_B = 90°$, $\phi_C = 180°$ and $\phi_D = 270°$), the opposite arms have current in the same direction but adjacent arms have a phase shift of 90°. This configuration makes SLA radiate two *H* components and two *V* components which add up in zenith but have a phase shift of 90° between them. This mode results in an axial beam of circular polarisation. Moreover, since the phase delay is from A to D, an LHCP beam is formed. Reversing the direction of phasing will form an RHCP beam. It should be noted that the final configuration of SLA is similar to that of various sequential patch antennas proposed in [17–19], which also produced axial beams. However, it is only the SLA which is capable of generating three distinct unit patterns (tilted, semi-doughnut and axial).

As described in [17], the mathematics of generating CP axial beam can also be explained if SLA is seen as analogous to a 2 × 2 array of microstrip antennas separated by a distance 2*d*, as shown in Fig. 10. The far field radiation pattern in the *xz*-plane and *yz*-plane can be obtained by vector summation

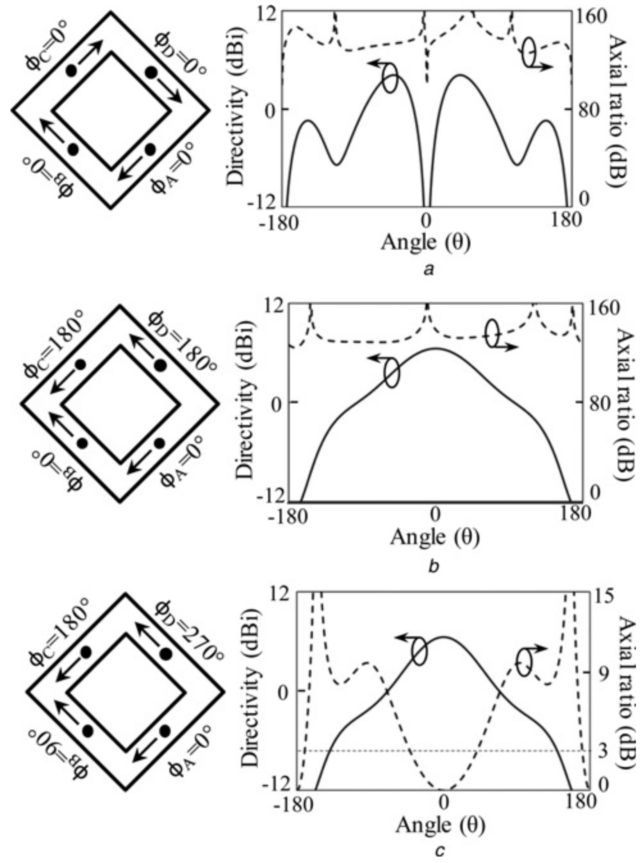

Fig. 9 *Direction of instantaneous currents and elevation cuts of radiation patterns and axial ratio of SLA at 4.7 GHz*

a $\phi_A = 0°$, $\phi_B = 0°$, $\phi_C = 0°$ and $\phi_D = 0°$
b $\phi_A = 0°$, $\phi_B = 0°$, $\phi_C = 180°$ and $\phi_D = 180°$
c $\phi_A = 0°$, $\phi_B = 90°$, $\phi_C = 180°$ and $\phi_D = 270°$

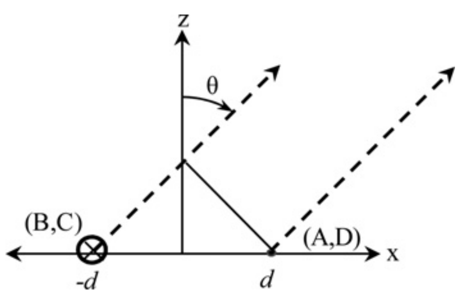

Fig. 10 *Geometrical layout of 2 × 2 array antenna analogy of SLA*

doi: 10.1049/iet-map.2012.0093

of the fields from all the four arms of the SLA. Let the resultant field in xz-plane is E_{xz}. Assuming the vertical field vectors from arms A and C as V_A and V_C and the horizontal filed vectors from arm B and D as H_A and H_D, respectively, the total far field can be given as

$$E_{xz} = V_A e^{j\beta\, d \sin\theta} e^{j0^\circ} + H_B e^{-j\beta\, d \sin\theta} e^{j90^\circ} - V_C e^{-j\beta\, d \sin\theta} e^{j180^\circ} - H_D e^{j\beta\, d \sin\theta} e^{j270^\circ} \quad (1)$$

As, $e^{j180^\circ} = -e^{j0^\circ}$ and $e^{j270^\circ} = -e^{j90^\circ}$ The total field E_{xz} becomes

$$\begin{aligned} E_{xz} &= V_A e^{j\beta\, d \sin\theta} e^{j0^\circ} + H_B e^{-j\beta\, d \sin\theta} e^{j90^\circ} \\ &\quad + V_C e^{-j\beta\, d \sin\theta} e^{j0^\circ} + H_D e^{j\beta\, d \sin\theta} e^{j90^\circ} \\ &= \left(V_A e^{j0^\circ} + H_D e^{j90^\circ}\right) e^{j\beta\, d \sin\theta} \\ &\quad + \left(V_C e^{j0^\circ} + H_B e^{j90^\circ}\right) e^{-j\beta\, d \sin\theta} \end{aligned} \quad (2)$$

Since all the four ports are excited by a signal of equal amplitude, $V_A = V_C = V$ and $H_B = H_D = H$ and

$$\begin{aligned} E_{xz} &= \left(V e^{j0^\circ} + H e^{j90^\circ}\right)\left(e^{j\beta\, d \sin\theta} + e^{-j\beta\, d \sin\theta}\right) \\ &= \left(V e^{j0^\circ} + H e^{j90^\circ}\right)\left\{2\cos\left(\beta d \sin\theta\right)\right\} \\ &= \left(V e^{j0^\circ} + H e^{j90^\circ}\right) \times \text{Array factor(AF)} \end{aligned} \quad (3)$$

The first term represents the pure LHCP wave and second term is the array factor of two element array. The array factor is the function of scanning angle θ and the distance d from the center of array and can be given as

$$\text{AF} = 2\cos(\beta d \sin\theta) = 2\cos(\psi) \quad (4)$$

where, $\psi = \beta d \sin\theta$

The principal maxima in array factor occurs when, $\psi = 0$

$$\begin{aligned} &\text{or} \quad \beta d \sin\theta = 0 \\ &\text{or} \quad \frac{2\pi}{\lambda_0} \times \frac{\lambda_0}{6} \times \sin\theta = 0 \\ &\text{or} \quad \theta = \sin^{-1}(0) = 0^0 \end{aligned} \quad (5)$$

It implies that the resultant radiated electric field has the maximum radiation at $\theta = 0°$, that is, directed along the z-axis ($z = 0$) and this accounts for the generation of axial beam.

5 Conclusion

An SLA over HHIS with simultaneous four port feeding network is presented for generation of a CP axial beam pattern. A complete feeding network integrated with the SLA over HHIS antenna was simulated and fabricated. Also, antenna characteristics are measured to cross validate the simulated results with the experimental results. The antenna operates at frequency band from 4.3 to 5 GHz, radiates a CP axial beam and has a maximum directivity of 7.4 dBi along z-axis. Finally, using current distributions it shown that single SLA can generate three distinct patterns.

6 References

1 Balanis, C.A.: 'Antenna theory' (John Wiley & Sons, Hoboken, New Jersey, 2005)

2 Pozar, D.: 'Finite phased arrays of rectangular microstrip patches', *IEEE Trans. Antennas Propag.*, 1986, **34**, (5), pp. 658–665

3 Jung, C.W., Lee, M., Li, G.P., De, F.F.: 'Reconfigurable scan-beam single-arm spiral antenna integrated with RF-MEMS switches', *IEEE Trans. Antennas Propag.*, 2006, **54**, pp. 455–463

4 Huff, G.H., Bernhard, J.T.: 'Integration of packaged RF MEMS switches with radiation pattern reconfigurable square spiral microstrip antennas', *IEEE Trans. Antennas Propag.*, 2006, **54**, pp. 464–469

5 Mehta, A., Mirshekar-Syahkal, D., Nakano, H.: 'Beam adaptive single arm rectangular spiral antenna with switches', *IEE Proc. Microw. Antennas Propag.*, 2006, **153**, (1), pp. 13–18

6 Mehta, A., Mirshekar-Syahkal, D., Nakano, H.: 'Pattern reconfigurable spiral antenna and its current distribution', *Microw. Opt. Technol. Lett.*, 2007, **49**, pp. 2567–2570

7 Mehta, A., Mirshekar-Syahkal, D.: 'Pattern steerable square loop antenna', *IEE Electron. Lett. (IET)*, 2007, **43**, (9), pp. 491–493

8 Pal, A., Mehta, A., Mirshekar-Syahkal, D., Messy, P.J.: 'Short-circuited feed terminations on beam steering square loop antennas', *IEE Electron. Lett. (IET)*, 2008, **44**, (24), pp. 1389–1390

9 Deo, P., Mehta, A., Mirshekar-Syahkal, D., Messy, P.J., Nakano, H.: 'Thickness reduction and performance enhancement of steerable square loop antenna using hybrid high impedance surface', *IEEE Trans. Antennas Propag.*, 2010, **58**, pp. 1477–1485

10 Kim, J.-Y., Lee, B., Jung, C.W.: 'Reconfigurable beam-steering antenna using double loops', *IEE Electron. Lett. (IET)*, 2011, **47**, (7), pp. 430–431

11 Deo, P., Pant, M., Mehta, A., Mirshekar-Syahkal, D., Nakano, H.: 'Implementation and simulations of commercial RF switch integration with steerable square loop antenna', *IEE Electron. Lett. (IET)*, 2011, **47**, (12), pp. 686–687

12 Pal, A., Mehta, A., Mirshekar-Syahkal, D., Nakano, H.: 'A square-loop antenna with 4-port feeding network generating semi-doughnut pattern for vehicular and wireless applications', *IEEE Antennas Wirel. Propag. Lett.*, 2011, **10**, pp. 338–341

13 Kraus, J.D., Marhefka, R.J.: 'Antennas' (McGraw-Hill, New York, 2003)

14 Hansen, R.C.: 'Evaluation of the large array method', *IEE Proc. Microw. Antennas Propag.*, 1990, **137**, (2), pp. 94–98

15 CST GmbH. Darmstadt, version 2011, Germany, Available at http://www.cst.com

16 SATIMO. Courtaboeuf, France

17 Huang, J.: 'A technique for an array to generate circular polarization with linearly polarized elements', *IEEE Trans. Antennas Propag.*, 1986, **34**, (9), pp. 1113–1124

18 Hall, P.S.: 'Application of sequential feeding to wide bandwidth, circularly polarised microstrip patch arrays', *Proc. Inst. Electr. Eng.*, 1989, **36**, Pt. H, (9), pp. 390–398

19 Jazi, M.N., Azarmanesh, M.N.: 'Design and implementation of circularly polarised microstrip antenna array using a new serial feed sequentially rotated technique', *IEE Proc. Microw. Antennas Propag.*, 2006, **153**, (2), pp. 133–140